



Progress

Meta-optics and bound states in the continuum

Kirill Koshelev^{a,b}, Andrey Bogdanov^b, Yuri Kivshar^{a,b,*}^a Nonlinear Physics Centre, Australian National University, Canberra ACT 2601, Australia^b ITMO University, St. Petersburg 197101, Russia

ARTICLE INFO

Article history:

Received 14 October 2018

Received in revised form 26 November 2018

Accepted 28 November 2018

Available online 8 December 2018

Keywords:

Bound states in the continuum

Meta-optics

Second-harmonic generation

Nanoresonator

Metasurfaces

ABSTRACT

We discuss the recent advances in meta-optics and nanophotonics associated with the physics of bound states in the continuum (BICs). Such resonant states appear due to a strong coupling between leaky modes in optical guiding structures being supported by subwavelength high-index dielectric Mie-resonant nanoantennas or all-dielectric metasurfaces. First, we review briefly very recent developments in the BIC physics in application to isolated subwavelength particles. We pay a special attention to novel opportunities for nonlinear nanophotonics due to the large field enhancement inside the particle volume creating the resonant states with high-quality (high-Q) factors, the so-called quasi-BIC, that can be supported by the subwavelength particles. Second, we discuss novel applications of the BIC physics to all-dielectric optical metasurfaces with broken-symmetry meta-atoms when tuning to the BIC conditions allows to enhance substantially the Q factor of the flat-optics dielectric structures. We also present the original results on nonlinear high-Q metasurfaces and predict that the frequency conversion efficiency can be boosted dramatically by smart engineering of the asymmetry parameter of dielectric metasurfaces in the vicinity of the quasi-BIC regime.

© 2018 Science China Press. Published by Elsevier B.V. and Science China Press. All rights reserved.

1. Introduction

The study of resonant dielectric nanostructures with large refractive index is a new research direction in nanoscale optics and metamaterial-inspired nanophotonics [1–3]. Many concepts of all-dielectric resonant nanophotonics are driven by the idea to employ subwavelength dielectric nanoparticles with Mie resonances as “meta-atoms” for creating highly efficient optical metasurfaces and metadevices [4]. Precise engineering of the optical resonances results in many fascinating phenomena such as perfect reflection, broadband transmission, complete control of phase and polarization, imaging with subwavelength resolution [5–8]. The pronounced resonant properties of high-index dielectric nanoparticles along with low-cost fabrication and compatibility with planar technology make high-index nanoscale structures prospective candidates to complement or even replace different plasmonic components in a range of potential applications. Moreover, many concepts which had been developed for plasmonic structures but could not be fully employed due to strong losses of metals, can now be realized based on low-loss dielectric structures.

High-index dielectric meta-atoms can support both electric and magnetic Mie resonances in the visible and mid-IR spectral ranges, which can be tailored by the nanoparticle geometry. To emphasize the importance of optically-induced magnetic response, the field of all-dielectric resonant nanophotonics is often termed as meta-optics. The study of Mie-resonant silicon nanoparticles have recently received considerable attention for applications in nanophotonics and metamaterials [9] including optical nanoantennas, wavefront-shaping metasurfaces, and nonlinear frequency generation. Importantly, the simultaneous excitation of strong electric and magnetic Mie-type dipole and multipole resonances can result in constructive or destructive interferences with unusual beam shaping [10], and it may also lead to the resonant enhancement of magnetic fields in dielectric nanoparticles that could bring many novel effects in both linear and nonlinear regimes.

The physics and applications of all-dielectric resonant nanophotonics could be extended substantially by employing the concept of bound states in the continuum (BICs), which represent localized states with energies embedded in the continuous spectrum of radiating waves. BICs were predicted as a mathematical curiosity in quantum mechanics long time ago [11]. In spite of the fact that the system proposed in that work has never been implemented experimentally, the beautiful physics of BIC was widely used, first in atomic physics [12–14] and then in acoustics and hydrodynamics [15–17]. For last years, BICs have been attracting very broad attention in photonics, primarily because they provide a simple

SPECIAL TOPIC: Electromagnetic Metasurfaces: from Concept to Applications.

* Corresponding author.

E-mail address: ysk@internode.on.net (Y. Kivshar).<https://doi.org/10.1016/j.scib.2018.12.003>

2095-9273/© 2018 Science China Press. Published by Elsevier B.V. and Science China Press. All rights reserved.

way to achieve very large quality factors (Q factors) for photonic crystals, metasurfaces, and even subwavelength isolated resonators. In part, the progress in the field of BICs before 2016 is covered in the review [18].

The key idea underlying bound states in the continuum is vanishing coupling between the resonant mode and all radiation channels of the surrounding space. Different BICs can be categorized with respect to the physical origin of radiation suppression; here, we follow the classification adopted from Ref. [18]. The coupling coefficient could vanish due to the symmetry reason when the spatial symmetry of the mode is incompatible with the symmetry of the outgoing radiating waves. Such kind of BIC is called symmetry-protected. It appears in a variety of photonic structures such as grating and metasurfaces, waveguide arrays, waveguides coupled to resonators, and many other [19–24]. In contrast to the symmetry-protected BIC, there is a so-called accidental BIC forming due to accidental vanishing of the coupling coefficients to the radiation waves via continuous tuning of one or several system parameters. The simplest example of accidental BIC is a Fabry-Pérot-type BIC. Such a state is formed between two mirrors resonantly reflecting the waves placed at a proper distance providing the phase shift multiple of 2π after the round-trip [25–27]. Some of accidental BICs could be explained in terms of destructive interference of two (or more) leaky waves, whose radiation is tuned to cancel each other completely. This mechanism is known as Friedrich-Wintgen scenario [14]. There are more specific examples of BIC arising, for example, in anisotropic [28], Floquet [29] or PT-symmetric systems [30,31]. Today the structures with optical BICs are successfully used for filtering, lasing, sensing and Raman spectroscopy [32–38]. Application of BICs for nonlinear optics, twisted light and light-matter interaction is under active study [22,24,27,39–43].

In practice, infinitely high Q factors of BICs are limited by a finite size of samples, material absorption, structural disorder and surface scattering [24,44]. As a result, BICs are transformed into states with a giant Q factor often treated as quasi-BICs. Remarkably, quasi-BICs can form even in a single subwavelength high-index dielectric resonator by tuning the structure parameters into the so-called supercavity regime [45–47]. In connection with broader applications, many metasurfaces composed of arrays of dissimilar meta-atoms with a broken in-plane symmetry can support high- Q resonances directly associated with the concept of quasi-BICs [48–50]. This includes, in particular, broken-symmetry Fano dielectric metasurfaces for enhancement of nonlinear effects [51] and recently reported biosensing with pixelated dielectric metasurfaces [52]. Currently, quasi-BICs in all-dielectric metasurfaces have been shown to be advantageous for a wide span of applications, including lasing [35,36], active photonics [53], polaritonics [42] and biophotonics [37,38]. The similar approach was proposed earlier for photonic-crystal slabs studied earlier with different applications in mind [54,55].

The aim of this paper is twofold. First, we summarize briefly very recent advances in the physics of bound states in the continuum in application to isolated subwavelength particles. We pay a special attention to novel opportunities for nonlinear nanophotonics due to the fact that high- Q states (quasi-BICs) supported by subwavelength particles are associated with large energy concentration inside the particle volume. Second, we discuss the application of these ideas to the physics of optical metasurfaces with broken-symmetry meta-atoms when tuning to the BIC conditions allows to enhance substantially the Q factor of the structure. In this section, we also present the original results about nonlinear high- Q metasurfaces and predict that the frequency conversion efficiency can be boosted dramatically by smart engineering the asymmetry parameter of dielectric metasurfaces in the vicinity of the quasi-BIC.

2. Isolated nanoparticles

To date, the nanoscale confinement of light and high Q factor of a resonator are crucial for many applications in photonics. Conventional ways to enlarge the Q factor are to increase the size of a resonator, for example, by exploiting whispering gallery modes and cavities in photonic crystals, or to arrange several resonators in space and excite collective modes. Although such techniques allow for light trapping with reduced energy losses, the size of the resonating system is still large compared to the operating wavelength. Recently, a completely different approach was proposed based on the concepts of BICs and supercavity modes which allows for subwavelength light confinement in all-dielectric high- Q resonators [45,56]. Such a mechanism of dramatic suppression of radiative losses for one of the interacting leaky modes is identical to emergence of accidental BICs in unbound structures, which originate in accord with the Friedrich-Wintgen scenario, when the radiating tails of several leaky modes cancel each other out via destructive interference resulting in a growth of the Q factor.

Fig. 1 summarizes the physics of the quasi-BIC formation in isolated subwavelength high-index resonators. The geometry of a nanoparticle is shown in Fig. 1a, being a nanodisk made of $\text{Al}_{0.2}\text{Ga}_{0.8}\text{As}$ suspended in a homogeneous background with refractive index 1. The values of permittivity and loss of AlGaAs are imported from the tabulated data [58] for the wavelength range around 1,600 nm.

The eigenmodes of a finite-length nanodisk can be roughly divided into two families, namely, radially oscillating and axially oscillating modes. Hereinafter, we call radial resonances originating from resonances of an infinitely long cylinder as Mie-like modes and axial modes – as Fabry-Pérot-like (FP-like) modes. A pair of low-frequency FP-like and Mie-like modes undergoes strong coupling via continuous tuning of the disk aspect ratio r/h producing the characteristic avoided resonance crossing feature, as shown in Fig. 1b. Since the nanodisk represents an open resonator, the radiative lifetime of interacting modes is also strongly modified [59] leading to the generation of a quasi-BIC with the enhancement of Q factor up to 120. This value is one order of magnitude higher than the Q factor of conventional dipolar resonances in the same frequency range.

The electric field profile and far-field distribution of the high- Q mode for the aspect ratio in- and out of the supercavity regime (see cases A, B, and C in Fig. 1b) are shown in Fig. 1c. It is clearly seen from the near-field distributions that a Mie-like mode smoothly transforms to a FP-like mode through a quasi-BIC with a hybrid field distribution. The lower panel of Fig. 1c shows that away from the quasi-BIC condition the far-field distribution of the high- Q mode is dominated by the magnetic dipole contribution. Since both FP-like and Mie-like modes are characterized by the magnetic dipole radiation pattern, their hybridization leads to sufficient suppression of the magnetic dipole component enabling the next allowed multipole – a highly symmetric magnetic octupole term. Such a behaviour is in full agreement with the results of multipolar decomposition of the eigenmodes [56,57], which explains the physical nature of the Q factor enhancement.

The supercavity regime can be observed in the evolution of the scattering spectra with respect to the change of the aspect ratio of a high-index dielectric resonator which reveals the characteristic avoided crossing behaviour [45]. The predicted features were recently confirmed in the proof-of-concept microwave experiment with a plastic cylindrical vessel filled with water [56]. The reported Rabi splitting was about 100 MHz at the frequency of 1 GHz.

In addition to the ARC hallmark, the quasi-BIC manifests itself as an abrupt change of the lineshape of the high- Q mode. In particular, in a narrow vicinity of the supercavity mode, the conventional

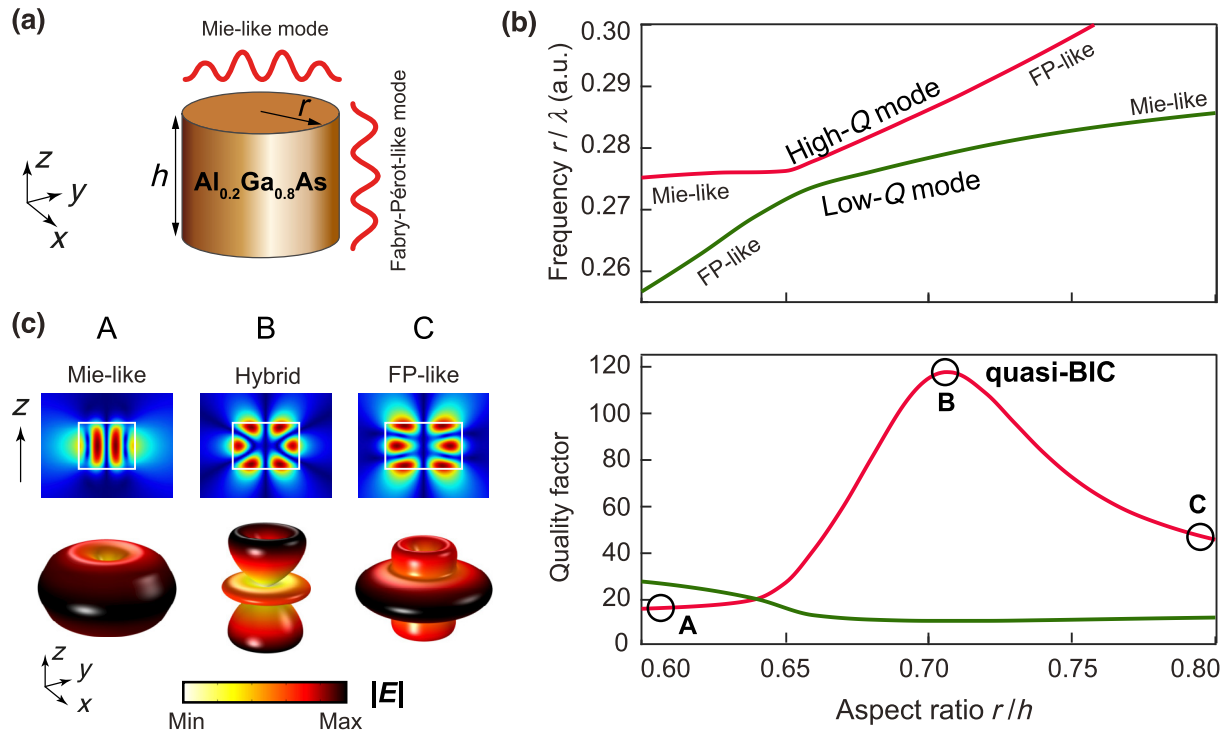


Fig. 1. (Color online) Quasi-BICs in isolated subwavelength nanoparticles. (a) Geometry of an AlGaAs cylindrical nanoparticle resonator with radius r and height h . (b) Strong coupling of two resonator modes resulting in the emergence of a quasi-BIC [45]. Upper panel: Mode frequencies vs. aspect ratio of the nanoparticle. Lower panel: Mode Q factor vs. aspect ratio. Points A, B, and C mark three regimes of the mode coupling, before and after the quasi-BIC supercavity condition is satisfied. (c) Upper panel: Near-field distributions of the electric field at the points A, B, and C. Lower panel: transformation of the radiation pattern for the high- Q mode while passing the avoided resonance crossing [56,57]. The quasi-BIC supercavity mode condition corresponds to the magnetic octupole mode.

Fano profile transforms into a symmetric Lorentzian peak. It results in a maximum of the scattering cross-section which is exactly opposite to the so-called anapole regime when the scattering becomes suppressed [60]. This transition can be analytically described by the peculiarities of the Fano asymmetry parameter which has different signs before and after the quasi-BIC condition, and it diverges when the quasi-BIC condition is satisfied [56]. Such a behavior is analogous to manifestation of BICs in unbound periodic structures, where the Fano parameter q becomes ill-defined corresponding to the “collapse” of Fano resonance [12]. Since the asymmetry of the Fano resonance is easily distinguishable without fitting, a quasi-BIC can be recognized in the experimental spectra. Thereby, the scattering spectra represent an unambiguous indicator of the supercavity regime in isolated subwavelength nanoparticles giving a deeper insight into the physics of BICs at the nanoscale.

A giant enhancement of the Q factor of dielectric nanoresonators is of a paramount interest for nonlinear optics, opening up new horizons for active and passive nanoscale metadevices. The reason is that nonlinear optics at the nanoscale is governed by strong field confinement and resonant response [61], and is not limited by phase matching [62]. As a result, the processes of high-order harmonic generation can be boosted dramatically since they scale as $(Q/V)^n$, where n is the process order and V is the mode volume [63]. Therefore, the giant increase of the generation efficiency is expected in isolated subwavelength nanoantennas tuned to the BIC regime which was recently predicted for the case of the second-harmonic generation (SHG) in AlGaAs nanodisks [64].

Fig. 2 outlines the results of our numerical analysis on the enhancement on the SHG efficiency for individual dielectric nanodisks in the supercavity regime. As shown in Fig. 2a, the resonator is excited by an azimuthally polarized Gaussian beam providing

perfect mode matching with the high- Q resonance, whose electric field is uniform with respect to the azimuthal direction (see Fig. 1c). The geometrical and material parameters of the disk are the same as were for the analysis of the linear response. For calculations, we assume the value of the beam waist equal to $1.5 \mu\text{m}$ and the value of the second-order nonlinear susceptibility equal to 290 pm/V [65].

Fig. 2b shows the intrinsic SHG conversion efficiency as a function of the disk aspect ratio, which is defined as P_{SH}/P_0^2 , where P_{SH} is the total power radiated at the second-harmonic frequency and P_0 is amount of the pump power actually coupled to the resonator. As it is shown, the SHG efficiency exhibits very dramatic growth in the vicinity of the supercavity mode, and it reaches its maximum exactly at the quasi-BIC condition. The additional boost of P_{SH} is provided by the resonant response of the disk at the frequency close to the quasi-BIC double frequency. The predicted record-high value of the conversion efficiency for nanoscale resonators exceeds by two orders of magnitude the conversion efficiency observed at the magnetic dipole Mie resonance [64].

In addition, we also notice that high- Q factors at the nanoscale can boost not only the sum-frequency generation efficiency, but also other processes, in particular, the spontaneous parametric downconversion. Recently, exploitation of the high- Q supercavity mode of the AlGaAs nanodisk was shown to produce a strong enhancement of generation of entangled photon pairs associated with electric and magnetic dipole modes [43].

3. Metasurfaces

Metasurfaces have attracted a lot of attention in the last years offering novel ways for wavefront shaping and advanced light

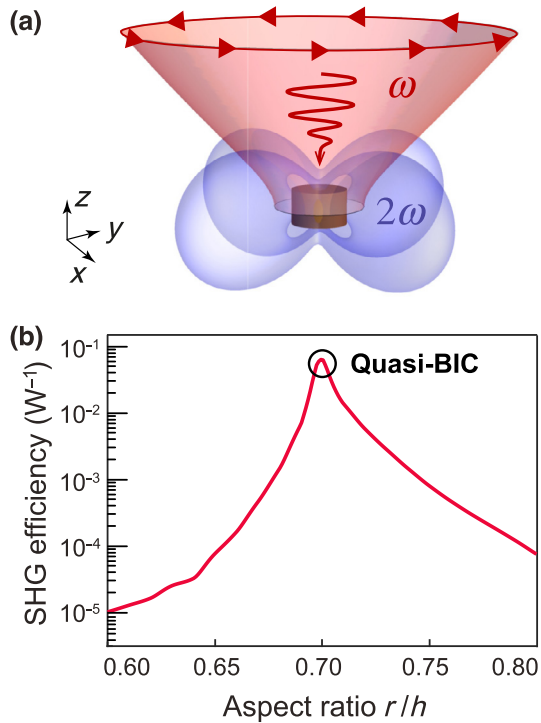


Fig. 2. (Color online) Enhanced SHG in the quasi-BIC regime. (a) Artistic view of the second-harmonic field generated from a subwavelength AlGaAs nanoantenna pumped by an azimuthally polarized beam at the BIC conditions. (b) Dependence of the intrinsic SHG conversion efficiency on the nanoparticle aspect ratio r/h with a large growth in the vicinity of the quasi-BIC [64]. An open circle corresponds to the maximum of the SHG efficiency, and it coincides with the conditions of the quasi-BIC regime.

focusing in combination with being ultra-thin optical elements [66–69]. Recently, metasurfaces based on high-index resonant dielectric materials have emerged as essential building blocks for various functional meta-optics devices [3] due to their low intrinsic loss, with unique capabilities for controlling the propagation and localization of light. A key concept underlying the specific functionalities of many metasurfaces is the use of constituent elements with spatially varying optical properties and optical response characterized by high Q factors of the resonances.

Recently, the resonant response of a special class of all-dielectric metasurfaces composed of meta-atoms with broken in-plane inversion symmetry was shown to demonstrate sharp resonances in the normal incidence reflection and transmission measurements. Such sharp Fano features are associated with modes possessing large Q factors which result in various unusual phenomena, including efficient imaging-based molecular barcoding [52] and enhanced nonlinear response [51]. In a very recent paper it was proven that all high- Q resonances in such seemingly different metasurfaces with asymmetric unit cells can be unified by the BIC concept [48]. In particular, it was validated that each sharp resonance originates from a symmetry-protected BIC which transforms to a quasi-BIC due to breaking of the in-plane inversion symmetry. More specifically, it was shown that the unit cell asymmetry induces an imbalance of the interference between contra-propagating leaky waves comprising the symmetry-protected BIC that leads to radiation leakage.

Fig. 3 combines the main results on the quasi-BIC formation in metasurfaces with broken in-plane inversion symmetry. Aiming further analysis of nonlinear resonant properties, we propose an original design of a square lattice metasurface with parallel dielectric bars of a slightly different width, as shown in Fig. 3a. The metasurface is made of $\text{Al}_{0.3}\text{Ga}_{0.7}\text{As}$, and it is placed on a fused quartz substrate; all material properties include losses being imported

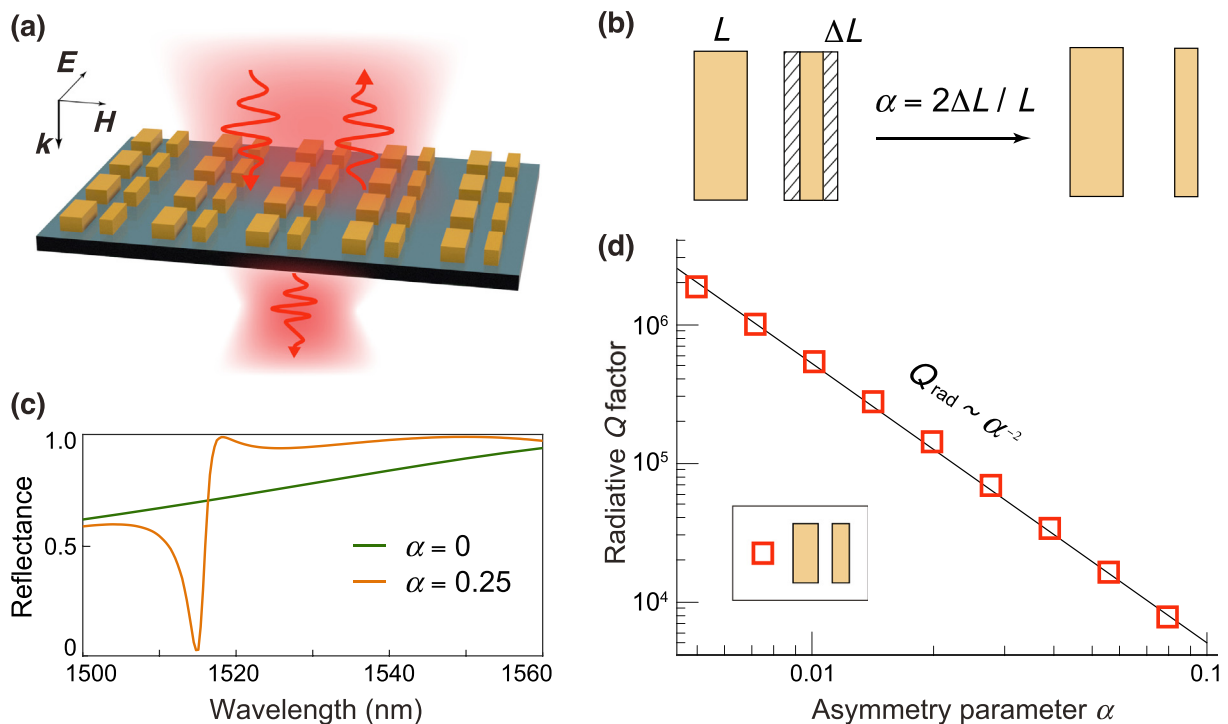


Fig. 3. (Color online) Quasi-BIC in metasurfaces with a broken symmetry. (a) Schematic of the scattering of light by an asymmetric metasurface composed of a square lattice of pairs of AlGaAs dielectric bars of different widths. Parameters are: period 950 nm, bar length 505 nm, bar width 250 nm, bar height 400 nm, and the distance between adjacent bars is 200 nm. (b) Definition of the asymmetry parameter α . (c) Evolution of the reflectance spectrum of the metasurface from the symmetric geometry ($\alpha = 0$) to a broken-symmetry geometry ($\alpha = 0.25$). (d) Inverse quadratic dependence of the Q factor on the asymmetry parameter α (log-log scale) [48]. The insert shows the specific shape of the isolated asymmetric meta-atom.

from the tabulated data [70]. Fig. 3b introduces the definition of the asymmetry parameter α . Nonzero difference in bar widths results in emergence of a sharp Fano profile in the reflectance spectrum (see results of numerical calculations in Fig. 3c). Excitation beam is a normally incident plane wave linearly polarized along the bars. Fig. 3d shows that the linewidth of such a resonance and, consequently, the mode Q factor are straightforwardly controlled by the magnitude of α defined in Fig. 3b.

Remarkably, for relatively small values of α the dependence of the Q factor on the asymmetry parameter is inverse quadratic which is the universal law for all metasurfaces with broken in-plane symmetry of meta-atoms [48]. For structures with weak dispersion of material properties the operating wavelength and the Q factor of a resonant symmetry-broken metasurface can be controlled efficiently by tuning the asymmetry parameter combined with a geometric rescaling of the structure. As a result, the understanding of the BIC-inspired nature of high-Q resonances paves the way towards smart engineering of metasurfaces-on-demand required for various applications of linear and flat optics.

Similarly to the case of individual high-Q nanoantennas, the enlargement of Q factor for metasurfaces boosts the conversion efficiency of sum-frequency generation processes dramatically. Below we present original results on the SHG efficiency for an example of broken-symmetry all-dielectric metasurface. We focus on the design shown in Fig. 3 with the difference between bar widths equal to 35 nm ($\alpha = 0.14$) which results in quasi-BIC with the Q factor of 2,500. In practice, it is not necessary to make Q factor more than $f/\delta f$, where f and δf are the center frequency and the bandwidth of the incident pulse, respectively. In calculations we assume the value of 290 pm/V for the second-order nonlinear susceptibility [65].

The results for the enhancement of the SHG conversion efficiency in the quasi-BIC regime are summarized in Fig. 4. We again focus on the intrinsic conversion efficiency defined as for the case of isolated nanoparticles. The reflectance spectrum manifests a sharp Fano resonance at the wavelength of about 1,532 nm, as shown in Fig. 4a. The insets show the in-plane cross sections of the near field distribution of the quasi-BIC. Fig. 4b demonstrates a rapid growth of the SHG conversion efficiency as a function of the pump wavelength with a pronounced maximum at the wavelength of the quasi-BIC. The metasurface is also simultaneously tuned to support a high-order mode with Q factor of 70 at the wavelength of 767 nm which makes the structure to be double-resonant and provides extra boost of the SHG conversion efficiency. Further enhancement of the conversion efficiency is possible for even smaller values of the asymmetry parameter being limited only by the material losses and structural imperfections.

4. Conclusion and outlook

Resonant dielectric nanoparticles and metasurfaces provide an alternative solution to enhance the performance of many nanophotonic structures and metadevices employing metallic elements and plasmonics effects. The study of resonant dielectric meta-optics has become a new research direction in metamaterials and nanophotonics, and it is expected to complement or substitute some of the plasmonic components in a range of potential applications. The unique low-loss resonant behavior makes it possible to reproduce many subwavelength resonant effects already demonstrated in nanoscale plasmonics without essential energy dissipation.

However, dielectric nanostructures supporting optically-induced Mie-type electric and magnetic resonances open many novel opportunities associated with interference effects and strong mode coupling, in both isolated high-index dielectric photonic res-

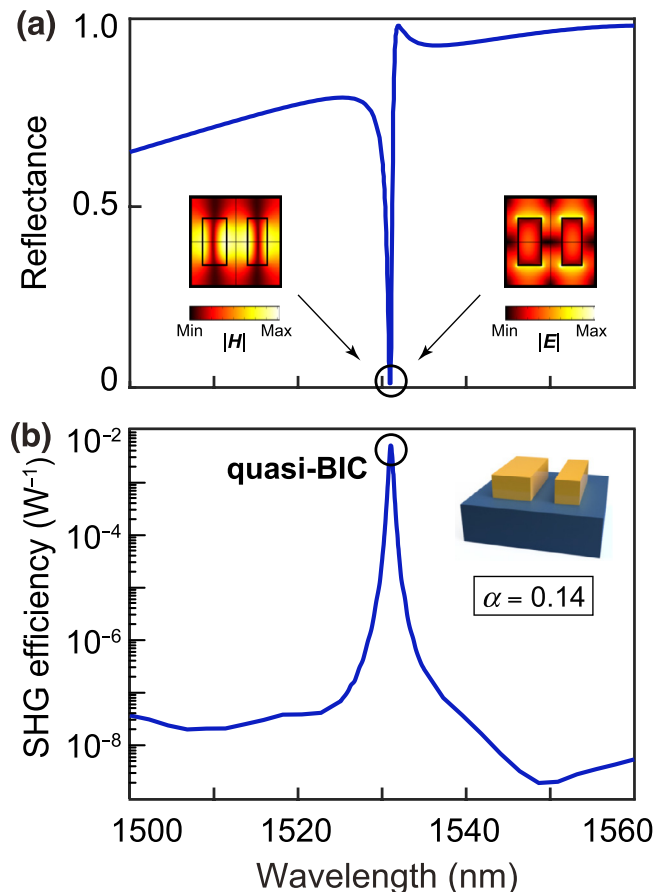


Fig. 4. (Color online) Nonlinear metasurfaces. Enhancement of the SHG conversion efficiency in broken-symmetry dielectric metasurfaces in the quasi-BIC regime. (a) Linear reflectance spectrum of the broken-symmetry metasurface with the parameters as in Fig. 3 and the difference in bar widths equal to 35 nm. The insets show the distribution of electric and magnetic fields of the excited quasi-BIC within the unit cell. (b) Dependence of the intrinsic SHG conversion efficiency on the pump wavelength calculated by nonlinear simulations. The open circle shows that the maximum of the SHG efficiency coincides with the quasi-BIC regime. The inset shows the specific shape of the metasurface unit cell.

onators and all-dielectric metasurfaces. The co-existence of strong electric and magnetic resonances, their interference, and the resonant enhancement of the magnetic response in dielectric nanoparticles bring new physics and entirely novel functionalities to simple geometries; a direction that has not been explored much so far, especially in the nonlinear regime.

A novel approach is associated with the bound states in the continuum which originate from strong coupling between the modes in resonant dielectric structures. They attracted a lot of attention in photonics recently as an alternative mean to achieve very large Q factors for lasing and also tune the system to the quasi-BIC supercavity regime. Importantly, even a single subwavelength high-index dielectric resonator can be tuned into the regime of a supercavity mode. This can be achieved by varying the nanoparticle's aspect ratio, when the radiative losses are almost suppressed due to the Friedrich-Wintgen scenario of destructive interference of leaky modes. In connection with broader applications, many metasurfaces composed of arrays of meta-atoms with broken in-plane symmetry can support high-Q resonances, which are directly associated with the concept of bound states in the continuum. This includes, in particular, broken-symmetry Fano dielectric metasurfaces for enhancement of nonlinear effects and recently reported pixelated dielectric metasurfaces for sensing. All such structures

can be employed in nonlinear nanophotonics, since they give rise to strong light-matter interaction on the nanoscale.

We believe that the novel approach to employ the BIC physics for enhancing the resonances in all-dielectric subwavelength structures and metasurfaces, and a recently proven direct link between the Fano resonances and quasi-BICs, provides a powerful tool to engineer the high-Q resonances and Purcell factors in nanoscale metadevices, allowing their numerous applications in sensing, nonlinear optics, quantum physics, and active nanophotonics.

Conflict of interest

The authors declare that they have no conflict of interest.

Acknowledgments

The authors thank Prof. Cheng-Wei Qiu for his kind invitation to contribute to this special topic, and they acknowledge productive collaboration and useful discussions with many colleagues and students, especially A. Alú, S. Kruk, S. Lepeshov, M. Limonov, Mingkai Liu, Wei Liu, Hong-Gyu Park, M. Rybin, D. Smirnova, and I. Staude. The authors acknowledge a financial support from the Australian Research Council, the Strategic Fund of the Australian National University and the Alexander von Humboldt Foundation. The part of the work related to single resonators was done with a financial support by the Russian Science Foundation (grant 18-72-10140). The part of the work related to metasurfaces was done with a financial support by the Ministry of Education and Science of the Russian Federation (3.1500.2017/4.6). K. K. and A. B. acknowledge the support from the Foundation for the Advancement of Theoretical Physics and Mathematics “BASIS” (Russia).

Author contributions

Kirill Koshelev performed the numerical studies. Andrey Bogdanov and Yuri Kivshar participated in the discussions of the results and the paper planning, and also contributed to the paper writing. Yuri Kivshar directed this project.

References

- [1] Kuznetsov AI, Miroshnichenko AE, Brongersma ML, et al. Optically resonant dielectric nanostructures. *Science* 2016;354:aag2472.
- [2] Staude I, Schilling J. Metamaterial-inspired silicon nanophotonics. *Nat Photonics* 2017;11:274–84.
- [3] Kruk S, Kivshar Y. Functional meta-optics and nanophotonics governed by Mie resonances. *ACS Photonics* 2017;4:2638–49.
- [4] Zheludev N, Kivshar Y. From metamaterials to metadevices. *Nat Mater* 2012;11:917–24.
- [5] Moitra P, Slovick BA, Li W, et al. Large-scale all-dielectric metamaterial perfect reflectors. *ACS Photonics* 2015;2:692–8.
- [6] Arbabi A, Horie Y, Bagheri M, et al. Dielectric metasurfaces for complete control of phase and polarization with subwavelength spatial resolution and high transmission. *Nat Nanotechnol* 2015;10:937.
- [7] Shalaev MI, Sun J, Tsukernik A, et al. High-efficiency all-dielectric metasurfaces for ultracompact beam manipulation in transmission mode. *Nano Lett* 2015;15:6261–6.
- [8] Yu YF, Zhu AY, Paniagua-Dominguez R, et al. High-transmission dielectric metasurface with 2π phase control at visible wavelengths. *Laser Photon Rev* 2015;9:412–8.
- [9] Kivshar YS. All-dielectric meta-optics and nonlinear nanophotonics. *Natl Sci Rev* 2018;5:144–58.
- [10] Liu W, Kivshar Y. Generalized Kerker effects in nanophotonics and meta-optics. *Opt Express* 2018;26:13085–105.
- [11] Von Neuman J, Wigner E. Concerning the behaviour of eigenvalues in adiabatic processes. *Phys Z* 1929;30:467–70.
- [12] Fonda L. Bound states embedded in the continuum and the formal theory of scattering. *Ann Phys* 1963;22:123–32.
- [13] Stillinger FH, Herrick DR. Bound-states in continuum. *Phys Rev A* 1975;11:446–54.
- [14] Friedrich H, Wintgen D. Interfering resonances and bound states in the continuum. *Phys Rev A* 1985;32:3231–42.
- [15] Ursell F. Trapping modes in the theory of surface waves. *Math Proc Cambridge Philos Soc* 1951;47:347–58.
- [16] Cumpsty NA, Whitehead DS. The excitation of acoustic resonances by vortex shedding. *J Sound Vib* 1971;18:353.
- [17] Parker R, Stoneman SA. The excitation and consequences of acoustic resonances in enclosed fluid flow around solid bodies. *Proc Inst Mech Eng C* 1989;203:9–19.
- [18] Hsu CW, Zhen B, Stone AD, et al. Bound states in the continuum. *Nat Rev Mater* 2016;1:16048.
- [19] Paddon P, Young JF. Two-dimensional vector-coupled-mode theory for textured planar waveguides. *Phys Rev B* 2000;61:2090–101.
- [20] Tikhodeev SG, Yablonskii AL, Muljarov EA, et al. Quasiguidded modes and optical properties of photonic crystal slabs. *Phys Rev B* 2002;66:045102.
- [21] Shipman SP, Venakides S. Resonant transmission near nonrobust periodic slab modes. *Phys Rev E* 2005;71:026611.
- [22] Bulgakov EN, Sadreev AF. Robust bound state in the continuum in a nonlinear microcavity embedded in a photonic crystal waveguide. *Opt Lett* 2014;17:5212–5.
- [23] Bulgakov E, Sadreev AF, Maksimov D. Light trapping above the light cone in one-dimensional arrays of dielectric spheres. *Appl Sci* 2017;7:147.
- [24] Belyakov MA, Balezin MA, Sadrieva V, et al. Experimental observation of symmetry protected bound state in the continuum in a chain of dielectric disks. *arXiv:1806.01932*; 2018.
- [25] Marinica DC, Borisov AG, Shabanov SV. Bound states in the continuum in photonics. *Phys Rev Lett* 2008;100:183902.
- [26] Ndagali RF, Shabanov SV. Electromagnetic bound states in the radiation continuum for periodic double arrays of subwavelength dielectric cylinders. *J Math Phys* 2010;51:102901.
- [27] Bulgakov EN, Pichugin KN, Sadreev AF. All-optical light storage in bound states in the continuum and release by demand. *Opt Express* 2015;23:22520–31.
- [28] Gomis-Bresco J, Artigas D, Torner L. Anisotropy-induced photonic bound states in the continuum. *Nat Photonics* 2017;11:232.
- [29] Zhong H-H, Zhou Z, Zhu B, et al. Floquet bound states in a driven two-particle Bose-Hubbard model with an impurity. *Chin Phys Lett* 2017;34:070304.
- [30] Longhi S. Bound states in the continuum in PT-symmetric optical lattices. *Opt Lett* 2014;39:1697–700.
- [31] Kartashov YV, Milián C, Konotop VV, et al. Bound states in the continuum in a two-dimensional PT-symmetric system. *Opt Lett* 2018;43:575–8.
- [32] Foley JM, Young SM, Phillips JD. Symmetry-protected mode coupling near normal incidence for narrow-band transmission filtering in a dielectric grating. *Phys Rev B* 2014;89:165111.
- [33] Liu Y, Weidong Z, Yuze S. Optical refractive index sensing based on high-Q bound states in the continuum in free-space coupled photonic crystal slabs. *Sensors* 2017;17:1861.
- [34] Romano S, Lamberti A, Masullo M, et al. Optical biosensors based on photonic crystals supporting bound states in the continuum. *Materials* 2018;11:526.
- [35] Kodigala A, Lepetit Th, Gu Q, et al. Lasing action from photonic bound states in continuum. *Nature* 2017;541:196–9.
- [36] Ha ST, Fu YH, Emani NK, et al. Directional lasing in resonant semiconductor nanoantenna arrays. *Nat Nanotechnol* 2018;13:1042.
- [37] Romano S, Zito G, Torino S, et al. Label-free sensing of ultralow-weight molecules with all-dielectric metasurfaces supporting bound states in the continuum. *Photonics Res* 2018;6:726–33.
- [38] Romano S, Zito G, Managó S, et al. Surface-enhanced Raman and fluorescence spectroscopy with an all-dielectric metasurface. *J Phys Chem C* 2018;122:19738–45.
- [39] Zhong H-H, Zhou Z, Zhu B, et al. Nonlinear bound states in the continuum of a one-dimensional photonic crystal slab. *Phys Rev B* 2018;97:224309.
- [40] Bulgakov EN, Sadreev AF. Bound states in the continuum with high orbital angular momentum in a dielectric rod with periodically modulated permittivity. *Phys Rev A* 2017;96:013841.
- [41] Bulgakov EN, Sadreev AF. Trapping of light with angular orbital momentum above the light cone. *Adv Electromagn* 2017;6:1–10.
- [42] Koshelev KL, Sychev SK, Sadrieva ZF, et al. Strong coupling between excitons in transition metal dichalcogenides and optical bound states in the continuum. *Phys Rev B* 2018;98:161113(R).
- [43] Poddubny AN, Smirnova DA. Nonlinear generation of quantum-entangled photons from high-Q states in dielectric nanoparticles. *arXiv:1808.04811*; 2018.
- [44] Sadrieva ZF, Sinev IS, Koshelev KL, et al. Transition from optical bound states in the continuum to leaky resonances: role of substrate and roughness. *ACS Photonics* 2017;4:723–7.
- [45] Rybin MV, Koshelev KL, Sadrieva ZF, et al. High-Q supercavity modes in subwavelength dielectric resonators. *Phys Rev Lett* 2017;119:243901.
- [46] Rybin M, Kivshar Y. Supercavity lasing. *Nature* 2017;541:164–5.
- [47] Taghizadeh A, Chung I-S. Quasi bound states in the continuum with few unit cells of photonic crystal slab. *Appl Phys Lett* 2017;111:031114.
- [48] Koshelev K, Lepeshov S, Liu M, et al. Asymmetric metasurfaces and high-Q resonances governed by bound states in the continuum. *Phys Rev Lett* 2018;121:193903.
- [49] Khardikov VV, Iarko EO, Prosvirnin SL. A giant red shift and enhancement of the light confinement in a planar array of dielectric bars. *J Opt* 2012;14:035103.
- [50] Zhang JF, MacDonald KF, Zheludev NI. Near-infrared trapped mode magnetic resonance in an all-dielectric metamaterial. *Opt Express* 2013;21:26721–8.

- [51] Campione S, Liu S, Basilio LI, et al. Broken symmetry dielectric resonators for high quality factor Fano metasurfaces. *ACS Photonics* 2016;3:2362.
- [52] Tittl A, Leitis A, Liu M, et al. Imaging-based molecular barcoding with pixelated dielectric metasurfaces. *Science* 2018;360:1105.
- [53] Han S, Cong L, Srivastava YK, et al. All-dielectric active photonics driven by bound states in the continuum. *arXiv:1803.01992;2018*.
- [54] Liang Y, Peng C, Sakai K, et al. Three-dimensional coupled-wave model for square-lattice photonic crystal lasers with transverse electric polarization: a general approach. *Phys Rev B* 2011;84:195119.
- [55] Zhou H, Zhen B, Hsu CW, et al. Perfect single-sided radiation and absorption without mirrors. *Optica* 2016;3:1079–86.
- [56] Bogdanov AA, Koshelev KL, Kapitanova PVV, et al. Bound states in the continuum and Fano resonances in the strong mode coupling regime. *arXiv:1805.09265;2018*.
- [57] Chen WJ, Chen YT, Liu W, Subwavelength high-Q Kerker supermodes with unidirectional radiations. *arXiv: 1808.05539;2018*.
- [58] Aspnes DE, Kelso SM, Logan RA, et al. Optical properties of $Al_xGa_{1-x}As$. *J Appl Phys* 1986;60:754–67.
- [59] Wiersig J. Formation of long-lived, scarlike modes near avoided resonance crossings in optical microcavities. *Phys Rev Lett* 2006;97:253901.
- [60] Miroshnichenko AE, Evlyukhin AB, Yu YF, et al. Nonradiating anapole modes in dielectric nanoparticles. *Nat Commun* 2015;6:8069.
- [61] Smirnova D, Kivshar YS. Multipolar nonlinear nanophotonics. *Optica* 2016;3:1241–55.
- [62] Kauranen M. Freeing nonlinear optics from phase matching. *Science* 2013;342:1182–3.
- [63] Notomi M. Strong light confinement with periodicity. *Proc IEEE* 2011;99:1768–79.
- [64] Carletti L, Koshelev K, De Angelis C, et al. Giant nonlinear response at the nanoscale driven by bound states in the continuum. *Phys Rev Lett* 2018;121:033903.
- [65] Shoji I, Kondo T, Kitamoto A, et al. Absolute scale of second-order nonlinear-optical coefficients. *J Opt Soc Amer B* 1997;14:2268–94.
- [66] Yu N, Capasso F. Flat optics with designer metasurfaces. *Nat Mater* 2014;13:139–50.
- [67] Kruk S, Hopkins B, Kravchenko II, et al. Broadband highly efficient dielectric metadevices for polarization control. *APL Photonics* 2016;1:030801.
- [68] Wang S, Wu PC, Su Vi-C, et al. Broadband achromatic optical metasurface devices. *Nat Commun* 2017;8:187.
- [69] Wang S, Wu PC, Su Vi-C, et al. A broadband achromatic metalens in the visible. *Nat Nanotechnol* 2018;13:227.
- [70] Aspnes DE, Kelso SM, Logan RA, Bhat R. Optical properties of $Al_xGa_{1-x}As$. *J Appl Phys* 1986;60:754–67.



Kirill Koshelev is a Ph.D. student at the Nonlinear Physics Centre, Australian National University. He received his M.S. degree in 2017 from the Academic University, Russia. His major research interest is in the field of theoretical analysis and designing of photonic nanostructures, nonlinear frequency generation, and bound states in the continuum.



Andrey Bogdanov received his Ph.D. degree in 2012 from the Ioffe Institute, Russia in the field of quantum cascade lasers. He is a postdoctoral fellow at the ITMO University, Russia. His current research efforts focus on theoretical investigation of optical nanoresonators and microcavities, bound states in the continuum and surface waves in metasurfaces.



Yuri Kivshar is a full-time professor and Head of Nonlinear Physics Centre at the Australian National University. He is Fellow of Australian Academy, AIP, OSA, APS, and IOP. Prof. Kivshar is a world leader in nonlinear physics, nonlinear photonics, and physics of metamaterials. In the last few years, his research focuses on meta-optics and all-dielectric nanophotonics with special interest to nonlinear, active and topological phenomena at the nanoscale.